ELSEVIER

Physica C 377 (2002) 1–6

PHYSICA C

www.elsevier.com/locate/physc

SEM, STM/STS and heavy ion irradiation studies on magnesium diboride superconductor

H. Narayan [a,*], S.B. Samanta [a], A. Gupta [a], A.V. Narlikar [a,1], R. Kishore [a], K.N. Sood [a], D. Kanjilal [b], T. Muranaka [c], J. Akimitsu [c]

[a] *National Physical Laboratory, Dr. K.S. Krishnan Marg, New Delhi 110 012, India*
[b] *Nuclear Science Centre, P.O. Box 10502, Aruna Asaf Ali Marg, New Delhi 110 067, India*
[c] *Department of Physics, Aoyama-Gakuin University, Setagaya-ku, Tokyo 157-8572, Japan*

Received 18 October 2001; received in revised form 11 December 2001; accepted 26 December 2001

Abstract

We have presented here the results of SEM and STM/STS investigations carried out on MgB_2 superconductor. The SEM pictures show porous surface and well-linked granular structure in which bigger grains (few micrometer size) seem to be agglomeration of smaller, nearly hexagonal grains (size nearly 100 nm). Hexagonal structure of Mg and B layers have been directly observed in atomically resolved STM images. The lattice constants have been determined to be $a_{Mg} = 3.1$ Å, $a_B = 1.7$ Å and $c = 3.5$ Å. Grain boundaries (GB) of width ranging from 50 to 200 Å have been observed. Absence of weak link effects despite wide GBs has been attributed to the metallic nature of the amorphous region of the GB interior as inferred from STS analysis. Irradiation with 200 MeV ^{107}Ag ions gives tracks of about 65 Å in the bulk of the sample. This is expected to give higher value of critical current density owing to the flux pinning mechanism, which is related to possibility of wide practical application of this material.

PACS: 74.70.Dd; 74.80.Bj; 68.37.Ef
Keywords: Magnesium diboride; Scanning electron microscopy; Scanning tunneling microscopy; Grain boundaries; Ion irradiation

1. Introduction

The recently discovered binary superconductor magnesium diboride (MgB_2) is a simple, intermetallic material with superconducting critical temperature T_c around 39 K [1,2]. For non-oxide, non-C_{60} based system, it is the highest observed T_c and therefore the discovery of superconductivity in this system has caused a lot of excitement in the world of material science. Immediately after the discovery, the very first question raised was which mechanism is responsible for superconductivity in this system. Although, most of the early experiments [2–7] suggested a phonon mediated cooper

* Corresponding author.
E-mail address: himnar@lycos.com (H. Narayan).
[1] Present address: Departamento de Fisica, Universidade Federal de Sao Carlos, Caixa Postal 676, 13565-905, Sao Carlos, Brazil.

0921-4534/02/$ - see front matter
PII: S0921-4534(02)01162-0

pair formation in superconducting MgB_2, some results did indicate differences from the BCS behaviour. Another interesting observation is the existence of a very sharp transition from normal to superconducting state [1] and the absence of weak link effects at the grain boundaries [8,9]. Moreover, the possibility of acquiring high values of critical current density (J_c) in high magnetic fields [8,9], which makes this material more suitable for technical applications, demands further investigation.

In an attempt to explain some of these strange behaviour, we report here the combined studies of scanning electron microscopy (SEM) and scanning tunneling microscopy/spectroscopy (STM/STS) carried out on MgB_2 system. Interestingly, this paper presents for the very first time, the direct observation of Mg and B hexagons using atomically resolved STM imaging. In addition, in light of the recent [10] results of an increased J_c in high fields achieved by producing atomic disorder by proton irradiation in MgB_2, we present the initial observation of columnar tracks in this system produced by 200 MeV ^{107}Ag ions irradiation.

2. Sample preparation and structure of MgB_2

The method of preparation of polycrystalline MgB_2 samples used in present work is reported elsewhere [1]. Resistivity and magnetic measurements confirmed the occurrence of superconductivity at 39 K in these samples. Analysis of XRD data assuming a hexagonal unit cell gives the values of lattice constant $a_{Mg} = 3.08$ Å. It is also known [1] that the Mg and B are arranged as hexagons in alternating planes separated by a distance 3.52 Å (c-axis separation).

SEM was carried out at ambient conditions using Leo 440 (Oxford Microscopy, England) instrument. At lower magnifications, SEM micrographs show presence of voids, which are expected in sintered samples, and also a well-linked granular structure (Fig. 1(a)). The linked structure of the grains seems to support the unhindered flow of supercurrent at lower temperature. Further, at higher magnifications, SEM shows (Fig. 1(b)) bigger grains (few micrometer in size) to be agglomerations of smaller grains (few 100 nm in size).

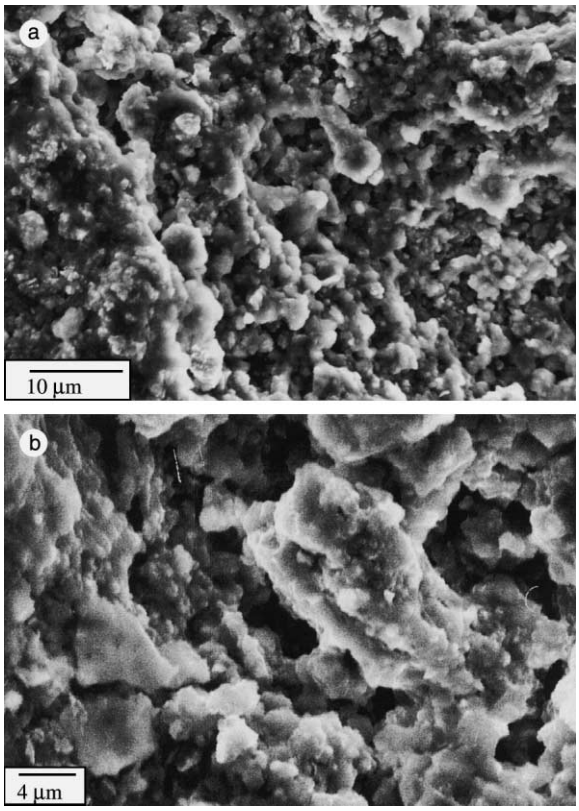

Fig. 1. (a) SEM photograph showing well linked granular structure in MgB_2. (b) Photograph at higher resolution showing the agglomeration of smaller grains into bigger ones.

STM has been carried out at ambient conditions using NanoScope II (Digital Instruments, USA) workstation operating in the constant current mode with bias voltage $V_b \approx -50$ mV. A Pt–Ir tip was used to scan the sample surface and data were collected with zero input filter and a moderate feedback gain. Typical results at atomic resolution showed the hexagonal configuration of Mg and B lattices. STM picture in Fig. 2(a) clearly shows the boron atoms arranged at the corners of smaller hexagon with magnesium atoms located at the centre. However, the central magnesium is not in the same plane but it is arranged as a larger close-packed hexagon in a different plane. Atomically resolved images of boron and magnesium

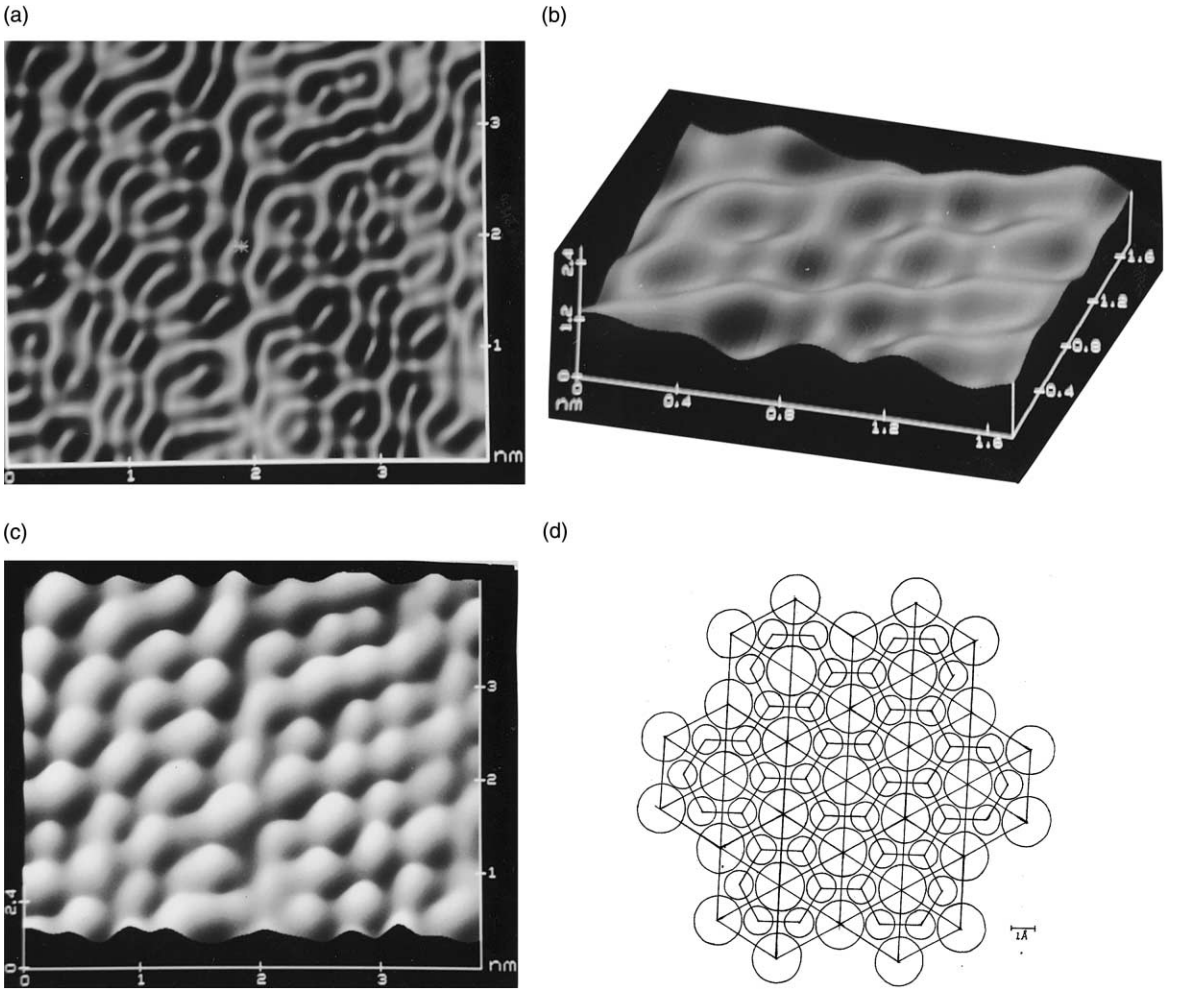

Fig. 2. (a) STM picture showing the hexagonal configuration of MgB_2 lattice. (Image in top view mode, scan size: 4 nm × 4 nm). (b) STM picture showing boron hexagons in MgB_2. (Image in 3D mode at 30° pitch, scan size: 1.7 nm × 1.7 nm). (c) STM picture showing magnesium hexagons in MgB_2. (Image in 3D mode at 60° pitch, scan size: 4 nm × 4 nm.) (d) Schematic diagram showing the structure of MgB_2 lattice. The bigger balls represent magnesium atoms whereas the smaller ones represent boron atoms.

hexagons are shown separately in 3D mode in Fig. 2(b) and (c), respectively. The length measurements carried out on the STM images give the values $a_{Mg} = 3.1$ Å and $a_B = 1.7$ Å. Schematic diagram of the structure of MgB_2 lattice, as visualized from STM, is shown in Fig. 2(d). The side view of the layered lattices is evident in the STM picture shown in Fig. 3. From this, the value of c has been determined to be equal to 3.5 Å. The lengths measured by us are therefore in good agreement with the already reported XRD results.

3. Nature of grain boundaries

Fig. 4 shows a typical STM image of a natural grain boundary (GB) of MgB_2, seen as a band of amorphous region separating two crystalline regions. Widths of GB measured in various STM pictures vary from 50 to 200 Å. Recently, even larger values of GB width (≈500 Å) have been obtained in HRTEM studies [11]. Such a large width of GB is normally expected to show weak-link effects. With a coherence length around

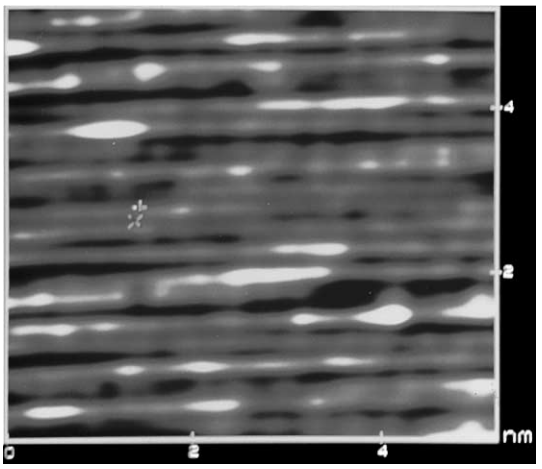

Fig. 3. STM picture showing side view of the layered lattice. (Image in top view mode, scan size: 5 nm × 5 nm.)

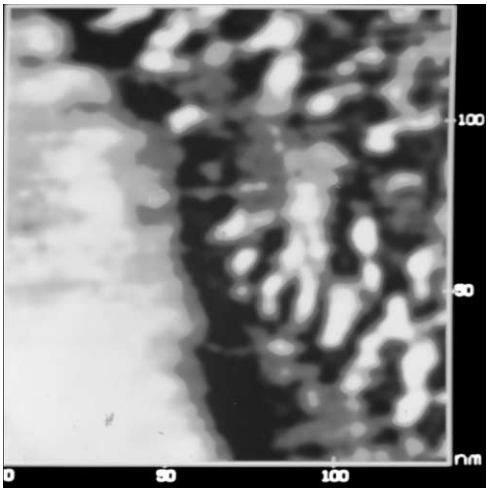

Fig. 4. STM picture showing one of the natural grain boundaries of MgB_2. (Image in top view mode, scan size: 130 nm × 130 nm.)

40–50 Å [12] in MgB_2, which is comparable only to the narrower regions of GB, wider regions are likely to support Joshephson weak link tunneling between adjacent grains. Consequently, J_c is expected to be significantly degraded near GB, and the transition from normal to superconducting state is expected to be broad. However, it is known [8,9], that J_c is not controlled by weak-link effects in MgB_2 and the transition is very sharp. These aspects have been further investigated by STS analysis.

After stabilizing the STM system for producing repetitive real time images of both grains and grain boundaries, scanning tunneling spectroscopy (STS) was switched on. For this, the feedback loop was opened for a fixed time, bias voltage was ramped and the change in tunneling current was measured as a function of the bias voltage. Using the software provided with the STM set up normalized conductance $\{(\partial I/\partial V)(V/I)\}$ was calculated and plotted simultaneously. The normalized conductance is a measure of local density of states (LDOS) and it changes sensitively from the characteristic V-shape to U-shape depending on whether the probed region is metallic or quasi-insulating in nature, respectively.

The evolution of normalized conductance, as the tip moves across one of the GB, can be seen in the STS spectra. Representative spectra taken in the middle of the GB and at the grain interior is shown in Fig. 5. The near V-shape of both the spectra reveals the metallic nature of amorphous region of GB as well as of the grain interiors. Finite non-zero value of normalized conductance for zero bias voltage, which is nearly constant as the STM tip moves across the grain boundary, implies that there is no significant change in LDOS [13]. This suggests that at temperatures below T_c the coupling between grains across GB is essentially S–N–S or proximity type instead of S–I–S type required for Joshephson weak links. The existence of such proximity coupling between the grains thus explains the absence of weak-link effect observed in this material. Further, the metallic nature of the amorphous regions of the GB does not seem unusual, as it is known [14] that semimetals (e.g. Bi, Ge, Si) do show metallicity in amorphous state and can even become superconducting.

4. Swift heavy ion irradiation induced effects

A sample of dimension 3 mm × 4 mm × 1 mm was irradiated at liquid nitrogen temperature by 200 MeV ^{107}Ag beam from the 15 UD pelletron accelerator at Nuclear Science Centre, New Delhi, up to a dose of 10×10^{10} ions/cm^2. The rate of electronic energy loss S_e and range R_p of this beam in the bulk of the sample were calculated using

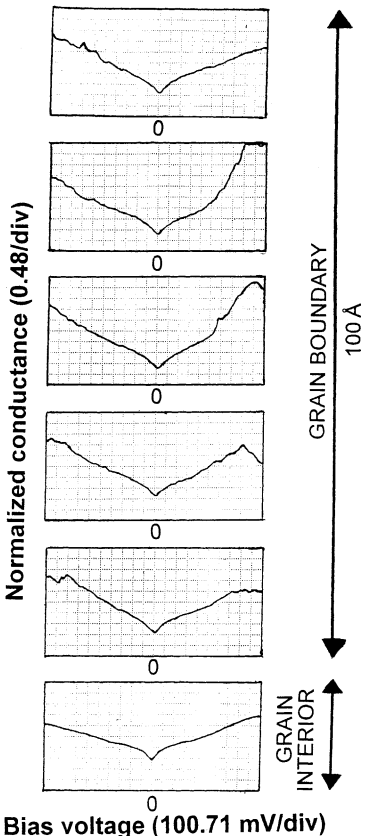

Fig. 5. Representative STS spectra taken at the grain interior and at the amorphous region of the grain boundaries (x-axis: bias voltage 100.71 mV/div, y-axis: normalized conductance 0.48/div).

Monte-Carlo SRIM simulation code [15]. The value of S_e is 1.85 keV/Å and that of R_p is about 15 μm. The nuclear energy loss (S_n) due to elastic collisions between the incident ions and the target atoms is negligibly small (less than three orders of magnitude than S_e) for MgB_2 submitted to 200 MeV ^{107}Ag ions. Hence the observed effects may be attributed entirely to S_e.

STM carried out on the irradiated surface shows amorphous tracks of diameter ranging from 50 to 80 Å (Fig. 6). Such a large value of track diameter suggests that columnar tracks should form in thin samples (thickness $< R_p$) under identical irradiation conditions. Considering that the average track diameter (around 65 Å) matches well with the estimated [12] coherence length (around

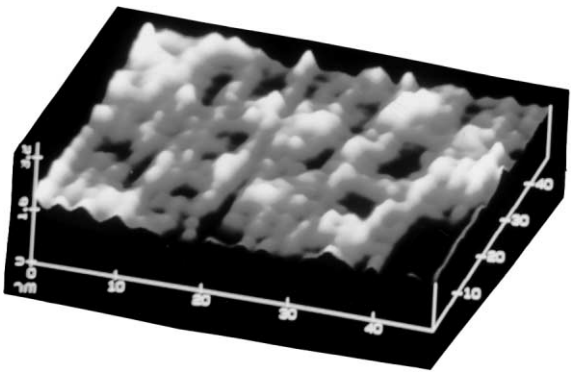

Fig. 6. STM picture showing the ion tracks created by 200 MeV ^{107}Ag ions in MgB_2. (Image in 3D mode at 30° pitch, scan size: 50 nm × 50 nm.)

45 Å), the columnar tracks can act as effective pinning centres for the flux vortices. Note that, since the columnar defects can pin the vortices all along its length, the expected increase in J_c can be even better than that observed recently by introducing point disorder in MgB_2 by proton irradiation [10].

STS measurements carried out as described above, on the amorphous tracks show metallic nature of the variation in normalized conductivity (Fig. 7). From the evolution of the STS curves, it is also evident that the LDOS decreases as the tip moves from edge towards centre of the track. Nevertheless, when compared with the STS plots taken at the GB, the STS plots of the tracks seem to be more V-shaped, i.e., more metallic. Further work regarding the nature of columnar tracks and their effects on J_c is in progress.

We conclude that the STM analysis of structure of MgB_2 provides an efficient method to directly observe the hexagonal configuration of the atomic arrangement. The lattice constants measured by us are in good agreement with the existing XRD results. STS analysis carried out at the GB reveals that the grains are linked with each other by proximity coupling which is expected to form S–N–S type junction below T_c and hence no weak link effect is caused. Irradiation with 200 MeV ^{107}Ag ions produces tracks of nearly 65 Å diameter which is expected to give columnar type defect in thin samples. Such defects may help in enhancing the high field J_c of the material making it more suitable for technological exploitation.

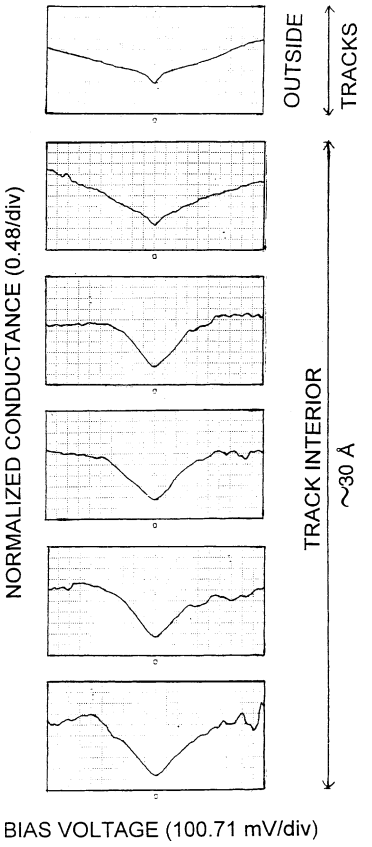

Fig. 7. Evolution of STS spectra taken at the interior of an ion track produced by 200 MeV ^{107}Ag ions irradiation of MgB_2, as the tip moves from one edge to the centre of the track. One representative spectra taken at the grain interior is also shown.

Acknowledgements

Part of this work was financially supported by CSIR grants (No.: 31/1/(179)/2000-EMR-I). The technical helps rendered by the staff at pelletron group at NSC, New Delhi, during irradiation experiments is also gratefully acknowledged. One of us (AVN), further thanks the emeritus scheme, CSIR, New Delhi.

References

[1] J. Nagamatsu, N. Nakagawa, T. Muranaka, Y. Zenitani, J. Akimitsu, Nature 410 (2001) 63–64.
[2] S.L. Bud'ko, G. Lapertot, C. Petrovic, C.E. Cunningham, N. Anderson, P.C. Canfield, Phys. Rev. Lett. 86 (9) (2001) 1877–1879.
[3] D.G. Hinks et al., Nature 411 (2001) 457.
[4] R.K. Kremer et al., cond-mat/0102432 (2001).
[5] Y. Wang et al., cond-mat/0103181 (2001).
[6] B. Lorenz et al., cond-mat/0102264 (2001).
[7] K. Kotegawa et al., cond-mat/0102334 (2001).
[8] D.C. Larbalestier, L.D. Cooley, M.O. Rikel, A.A. Polyanskii, J. Jiang, S. Patnaik, X.Y. Cai, D.M. Feldmann, A. Gurevich, A.A. Squitieri, M.T. Nans, C.B. Eom, E.E. Hellstrom, R.J. Cava, K.A. Regan, N. Rogado, M.A. Hayward, T. He, J.S. Slusky, P. Khalifah, K. Inumaru, M. Haas, Nature 410 (2001) 186–189.
[9] Y. Bugoslavski et al., Nature 410 (2001) 563–565.
[10] Y. Bugolavsky, L.F. Cohen, G.K. Perkins, M. Polichettl, Y.J. Tate, R. Gwilliam, A.D. Caplin, Nature 411 (2001) 561–565.
[11] Y. Zhu et al., Studies of High Temperature Superconductors, vol. 38, Nova Sci., NY, in press.
[12] H.H. Wen, cond-mat/0103521 (2001).
[13] S.B. Samanta, H. Narayan, A. Gupta, A.V. Narlikar, T. Muranaka, J. Akimitsu, Phys. Rev. B 65 (2002) 092510.
[14] A.V. Narlikar, S.N. Ekbote, Superconductivity and Superconducting Materials, South Asian Publishers, Delhi, 1983.
[15] J.F. Ziegler, J.P. Biersack, Stopping and Range of Ions in Matter, version: 97.09 1997. The Stopping and Range of Ions in Solids, Pergamon, New York, for further information and download see: Available from http://www.research.ibm.com/ionbeams/home.htm. The Stopping and Range of Ions in Matter, version: 97.09.